2019 SCEC Project Report * Project 19063
Temporal changes of seismicity in relation to preparation processes of large earthquakes and decade-scale climate changes

1. PROJECT SUMMARY

Improved understanding of fault resistance and partitioning of the ongoing loading among seismic and aseismic processes is recognized among the fundamental problems of earthquake physics by SCEC5. The goal of the current project was to quantify non-stationary aspects of seismicity, with a focus on dynamics of seismicity and preparation processes of large earthquakes.

Specifically, we proposed to work on a time-dependent version of previously developed spatial techniques, and apply them to the observed seismicity of southern California. The project goals included the following tasks:

Examine changes in earthquake patterns during preparation processes of large earthquakes in California. The analysis will include the Landers (1992, M7.3), Northridge (1994, M6.7), Hector Mine (1999, M7.1), and El Mayor Cucapah (2010, M7.2) earthquakes in southern California. We will also examine the Parkfield (2004, M6.0) earthquake in northern California, as a case of a relatively isolated natural system (rupture surrounded by creeping zones). The proposed analysis will focus on several alternative approaches to detecting localization of damage prior to a large event.

2. PROJECT RESULTS

Summary of results: The project developed a methodology for robust quantification of appearance and localization of earthquake damage prior to large earthquakes. The methodology has been tested in Southern California, the Parkfield section of San Andreas Fault, and Turkey [**Sect. 2.1**; *Ben-Zion and Zaliapin*, 2020]. The project examined different styles of earthquake clustering and earthquake repeaters in the Sea of Marmara, with implications to earthquake nucleation [**Sect. 2.2**; *Martinez-Garzon et al.*, 2019]. The project is using the nearest-neighbor declustering of *Zaliapin and Ben-Zion* [2020] as an essential part of its methodology. Finally, we started exploration of the hyperbolic geometry of the earthquake field, as a way of providing a background for the nearest-neighbor earthquake methodology developed and used in this project [**Sect. 2.3**; *Henricksen and Zaliapin*, 2019].

Project outcomes: The project results are presented in three peer-reviewed publications (two published, one in review), and multiple conference presentations.

2.1 Localization and coalescence of seismicity before large earthquakes [*Ben-Zion and Zaliapin*, in review, 2020]

We examine localization processes of low magnitude seismicity in relation to the occurrence of large earthquakes using three complementary analyses: (i) estimated production of rock damage by background events, (ii) evolving occupied fractional area of background seismicity, and (iii) progressive coalescence of individual earthquakes into

clusters. The different techniques provide information on different time scales and the spatial extent of weakened damaged regions. Techniques (i) and (ii) employ declustered catalogs to avoid the occasional strong fluctuations associated with aftershock sequences, while technique (iii) examines developing clusters in entire catalog data. We analyze primarily earthquakes around large faults that are locked in the interseismic periods, and examine also as a contrasting example seismicity from the creeping Parkfield section of the San Andreas fault. Results of analysis (i) show that the $M > 7$ Landers 1992, Hector Mine 1999 and Ridgecrest 2019 earthquakes in Southern California were preceded in the previous decades by generation of rock damage around the eventual rupture zones (**Fig. 1**). Analysis (ii) reveals localization (reduced fractional area) 2-3 yr before these $M > 7$ earthquakes, along with the $M > 7$ El Mayor-Cucapah 2010 earthquake in Baja CA and the Düzce 1999 earthquake in Turkey (**Figs. 2,3**). Results with technique (iii) indicate that individual events tend to coalesce rapidly to large clusters in the final 1-2 yr before the mainshocks. Corresponding analyses of data from the Parkfield region show opposite delocalization patterns and decreasing clustering before the 2004 M6 earthquake. Continuing studies with these techniques, combined with analysis of geodetic data and insights from laboratory experiments and model simulations, can improve the ability to track preparation processes leading to large earthquakes.

2.2 Earthquake clustering and earthquake repeaters in the Sea of Marmara: Implications for monitoring of earthquake nucleation [*Martinez-Garzon et al., Tectonophysics,* 2020]

Quantifying regional earthquake cluster style is essential for providing a context for studies of seismicity patterns and earthquake interactions. Here, we identify clusters of seismicity in the Sea of Marmara region of the North Anatolian Fault, NW Turkey, using a recently derived high-resolution seismicity catalog and the nearest-neighbor earthquake cluster approach. The detected earthquake clusters are utilized for (1) determining spatial distribution of mainshock and aftershock rates and estimating the proximity to failure on different fault segments, (2) identifying fault sections having earthquake repeaters, and (3) finding areas with enhanced foreshock activity. About 6%, 70% and 24% of the events are identified as foreshocks, mainshocks and aftershocks, respectively, with the largest concentration of aftershocks and foreshocks located along the Western High and the Cinarcik Fault, respectively. The method successfully identifies regions where previous studies reported earthquake repeaters as indicator for fault creep and suggests additional repeater areas in the Gulf of Gemlik. The largest proportion of mainshocks with associated foreshocks and aftershocks are along the Western High and Cinarcik Fault segments, potentially indicating that these segments are closer to failure and have increased susceptibility to seismic triggering. Continuing studies can contribute to monitoring possible preparation phase of a large ($M > 7$) earthquake in the Marmara region near the Istanbul Metropolitan region.

2.3 Hyperbolic Property of Earthquake Networks [*Henricksen and Zaliapin, JSM,* 2019]

We examine the geometry of earthquakes in time-space-magnitude domain using the Gromov hyperbolic property of metric spaces. Gromov delta-hyperbolicity quantifies the

curvature of a metric space via four-point condition, which is a computationally convenient analog of the famous slim triangle property. We estimate the delta-hyperbolicity for the observed earthquakes in Southern California during 1981-2017. A set of earthquakes is quantified by the Baiesi-Paczuski proximity η that has been shown efficient in applied cluster analyses of natural and human-induced seismicity and acoustic emission experiments. The Gromov delta is estimated in the earthquake space (D, η) and in proximity graphs obtained by connecting pairs of earthquakes within proximity η_0. All experiments result in the values of delta that are bounded from above and do not tend to increase as the examined region expands. This suggests that the earthquake field has hyperbolic geometry. We discuss the properties naturally associated with hyperbolicity in terms of the examined field. The results improve the understanding of dynamics of seismicity and further expand the list of natural processes characterized by the underlying hyperbolic geometry.

Project publications:

Published papers:

1. Zaliapin, I. and Y. Ben-Zion (2020) Earthquake declustering using the nearest-neighbor approach in space-time-magnitude domain. *J. Geophys. Res.* – Solid Earth, e53991. https://doi.org/10.1029/2018JB017120 [included in 2018 report]
2. Martínez-Garzón, P., Y. Ben-Zion, I. Zaliapin, and M. Bonhoff (2019) Earthquake clustering and earthquake repeaters in the Sea of Marmara: Implications for monitoring of earthquake nucleation. *Tectonophysics*, 768, 228176. https://doi.org/10.1016/j.tecto.2019.228176

Paper in review:

1. Zaliapin, I. and Y. Ben-Zion (2020) Localization and coalescence of seismicity before large earthquakes.

Conference abstracts/proceedings:

1. Zaliapin, I., K. Henricksen, and K. Zuev (2019) Hyperbolic geometry of earthquake networks. Abstract S54B-03 presented at *2019 Fall Meeting of AGU, Washington D.C.*, December 9-13, 2019.
2. Ben-Zion, Y. and I. Zaliapin (2019) Quantifying preparation process of large earthquakes: Damage localization and coalescent dynamics. Abstract S54B-01 presented at *2019 Fall Meeting of AGU, Washington D.C.*, December 9-13, 2019.
3. Zaliapin, I., and Y. Ben-Zion (2019). Quantifying preparation process of large earthquakes: Damage localization and coalescent dynamics. *Proc. of Southern California Earthquake Center (SCEC) 2019 Annual Meeting*, Palm Springs, CA, September 7-11, 2019, Vol. XXIX, poster 089.
4. Henricksen, K. and I. Zaliapin (2019) Hyperbolic property of earthquake networks. In JSM Proceedings, Statistics and the Environment Section. Alexandria, VA: American Statistical Association, 2024 – 2047.

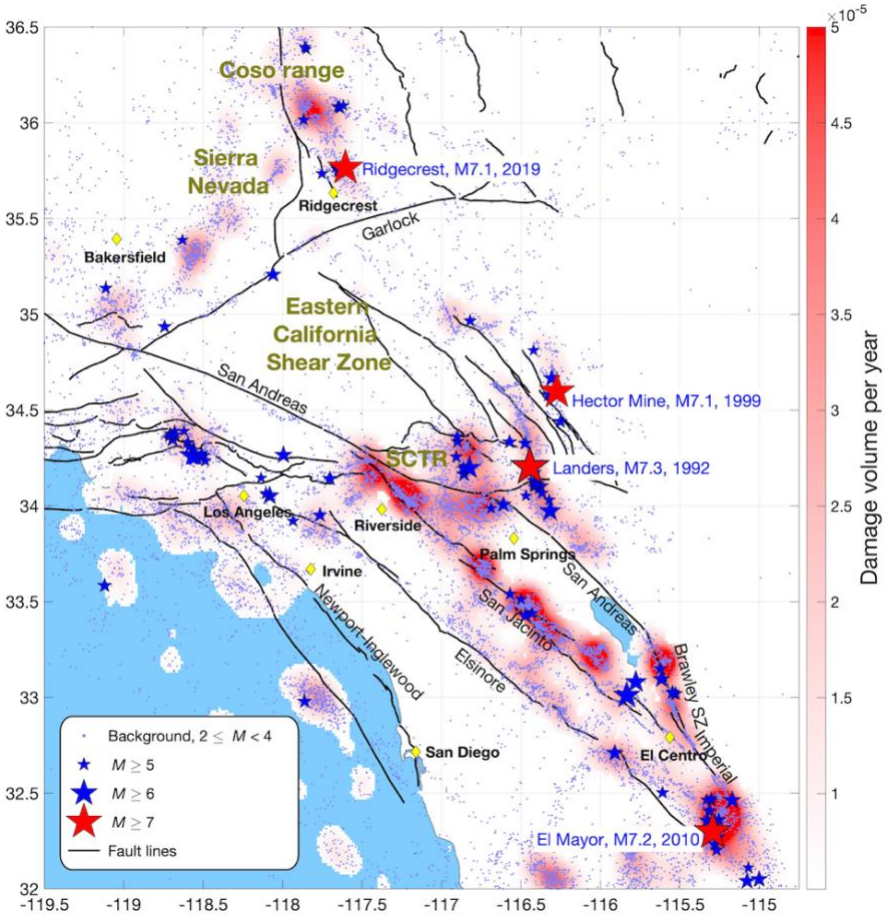

Figure 1: Estimated damage volume V in km^3 yr^{-1} (color code) projected at the earth surface. The damage is estimated using background events with magnitude $2 \leq M < 4$ during 1981 – 2019.5 shown by dots. The damage values are clipped at 5×10^{-5} and values below 5×10^{-6} are transparent.

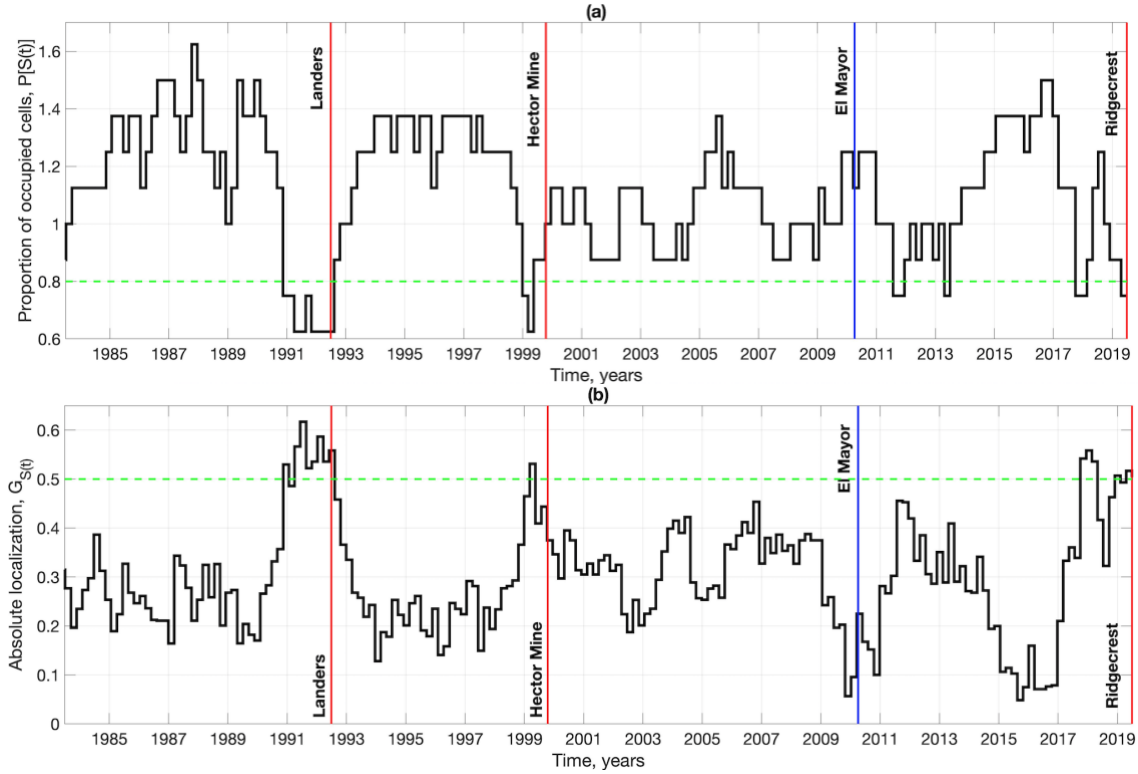

Figure 2: Premonitory localization of background events within Eastern Southern California. The times of the three largest ($M > 7$) earthquakes in the region are shown by vertical red lines. The time of the El Mayor-Cucapah event outside the examined region is shown by the vertical blue line. The analysis uses $M \geq 3$ background events, sliding time window of $\Delta t = 2.5$ yr, spatial cells with $\Delta\phi = 0.5°$, and threshold $S_0 = 20$. (a) Normalized proportion $P[S(t)]$. (b) Absolute localization $G_{S(t)}$. Green horizontal lines emphasize increased (panel a) or decreased (panel b) values of the examined statistic prior to the large earthquakes.

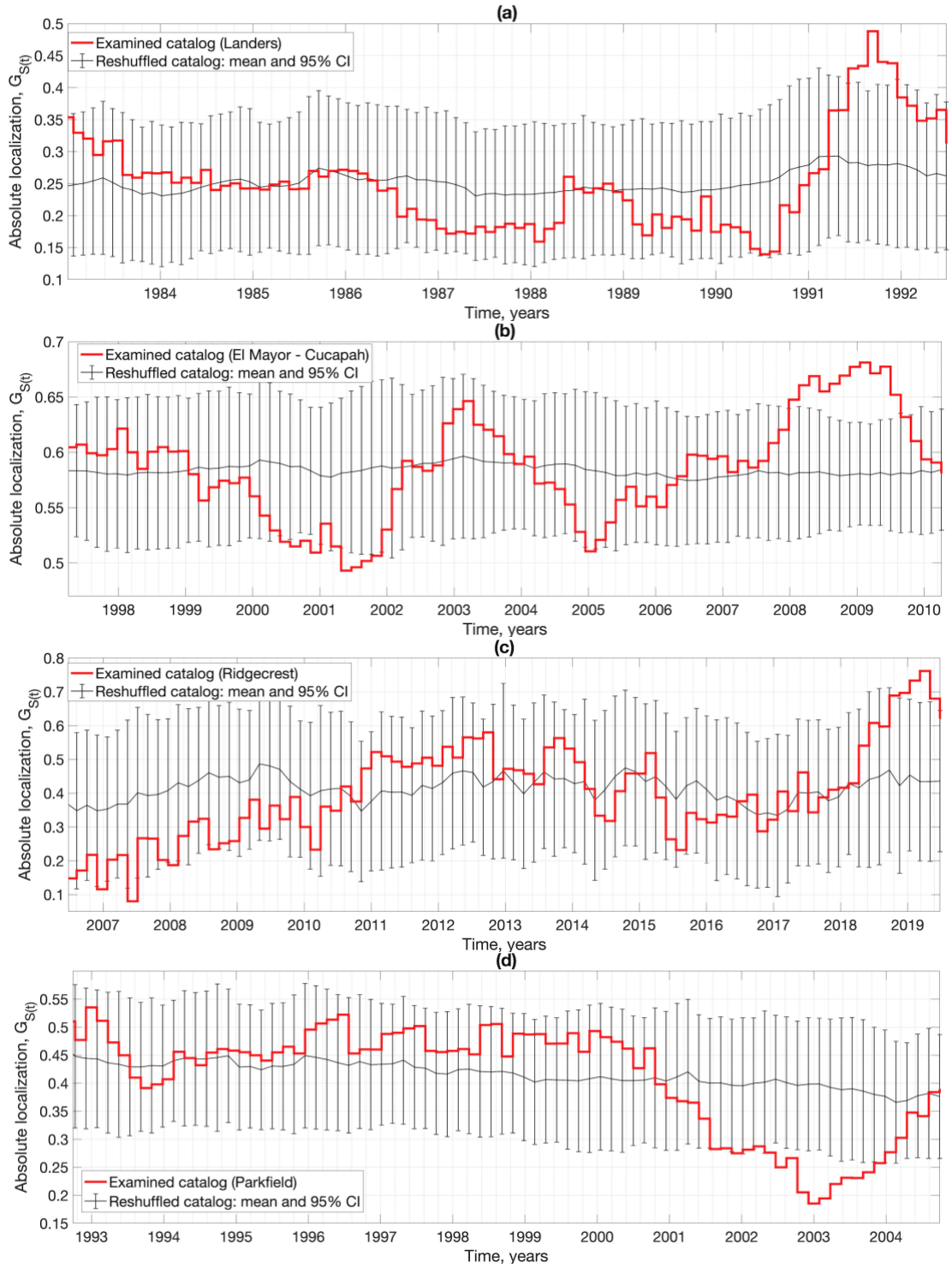

Figure 3: Absolute localization, $G_{S(t)}$, of background events before large earthquakes. Red – observations, black – reshuffled catalogs with simulated 95% confidence interval. (a) Landers, M7.3. (b) El Mayor-Cucapah, M7.2. (c) Ridgecrest, M7.1. (d) Parkfield, M6. Note the opposite trend (delocalization) prior to the M6 Parkfield event.